inter•noise 96
25th Anniversary Congress – Liverpool

INCE: 46

ANALYTICAL/EXPERIMENTAL STUDY OF VIBRATION OF A ROOM-SIZED AIRSPRING SUPPORTED SLAB

H Amick (1), B Sennewald (2), N C Pardue (2), C Teague (3) & B Scace (3)

(1) Acentech Incorporated, 21116 Vanowen Street, Canoga Park, California, USA, (2) Henningson Durham & Richardson Inc, 103 Oronoco Street, Alexandria, Virginia, USA, (3) National Institute of Standards and Technology (NIST), Gaithersburg, Maryland, USA

1. INTRODUCTION

Limiting the transmission of ambient vibration to sensitive experiments has been a long-standing need at the U.S. National Institute of Standards and Technology (NIST). One goal in the on-going design of the Advanced Technology Laboratories (ATLs) is to provide highly controlled vibration environments in laboratory spaces. Experience at European metrology laboratories suggested that the use of pneumatically supported concrete inertia slabs could permit achievement of this goal. NIST commissioned design and construction of a prototype slab of significant size (4 m x 10 m) using readily available vibration-isolation components.

This paper presents the results of a thorough study of the modal properties of the prototype slab using experimental methods and finite element modeling. The intent of the study was two-fold: (1) to document the dynamic characteristics of the prototype slab and (2) to determine the extent to which finite element modeling could be used as a design tool to predict slab behavior.

2. SLAB DESIGN PARAMETERS

Vibration Criterion. NIST scientists and the ATL design team agreed that an appropriate vibration criterion for the isolated slabs would be a velocity amplitude of 0.75 micrometers/sec (μm/s)—one-fourth of the typical on-grade velocity amplitude—at frequencies above the "skirt" of the airspring resonance curve, about 8 Hz.

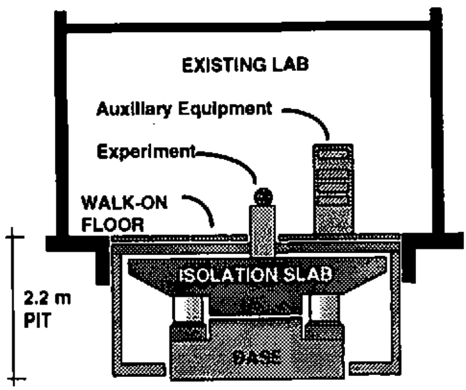

Figure 1. Section Through Laboratory and Slab.

The Slab and its Model. The slab was designed to fit in an existing pit in a laboratory space at NIST. This effectively defined limits on the size and aspect ratios that could be employed. In its final configuration, the isolated slab had a T-shaped cross section–a slab with a keel–as shown conceptually in Fig. 1. The slab depth is 600 mm; the keel adds another 300 mm. The slab is intended to support only vibration-sensitive apparatus; personnel and auxiliary experimental equipment are to be supported on an edge-supported "walk-on" floor. The isolated slab is supported on 10 commercially available airsprings rated to provide resonance frequencies of 1.5 Hz vertically and 3.1 Hz horizontally.

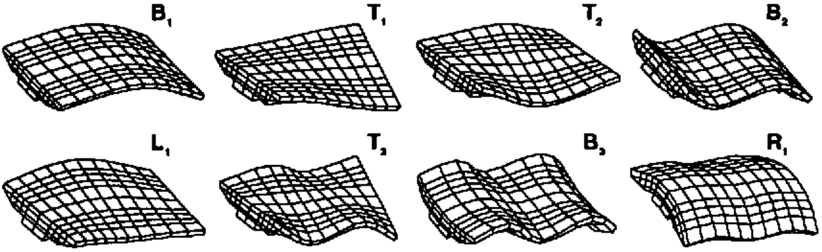

Figure 2. Calculated Modeshapes of Slab Deformation.

A finite element model (FEM) of the slab was constructed from 300 "solid" elements to represent the slab and 10 "beam" elements configured to simulate the stiffnesses of the airsprings. In addition, the concrete foundation beneath the slab was modeled using plate bending elements and the soil beneath the foundation was represented by massless spring elements. The entire FEM was implemented using GT-STRUDL®, a proprietary finite element software package.

3. SYSTEM RESONANCES

Calculated Modeshapes. The finite element model was used to calculate the modeshapes of the first 30 modes of the system. This set included 12 modes corresponding essentially to motion of the rigid mass on the airsprings and the foundation mass on the soil springs. The remaining 18 modes are associated predominantly with deformations of the slab. The first 8 of these modes had frequencies below 200 Hz, the limit of the range of interest for this study. The deformed shapes associated with these 8 modes are shown in Fig. 2. Because of its non-symmetric T-shaped cross-section, its deformations do not correspond to either "pure plate" or "pure beam" behavior. The labels B_1, B_2, and B_3 were used to denote the first three modes similar to beam bending; T_1, T_2, and T_3 to denote the first three modes similar to torsion of a prismatic section; L_1 to denote the first combined flexural-torsional mode; and R_1 to denote what might be called a "barrel" mode associated predominantly with bending about the longitudinal axis.

Figure 3. Velocity Spectra from Hammerblows

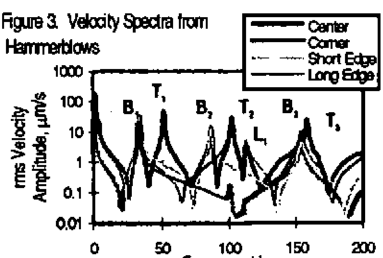

Table 1. Summary of Resonance Frequencies

Mode	Description	Frequency, Hz Predicted	Frequency, Hz Measured
B_1	First bending mode	33	34
T_1	First torsional mode	39	52
B_2	Second bending mode	84	87
T_2	Second torsional mode	80	102
L_1	Lateral-torsional mode	91	112
B_3	Third bending mode	150	154
T_3	Third torsional mode	128	158
R_1	Barrel mode	174	-

Hammerblow Response. A mallet was used to strike the slab at four locations, with exponentially averaged velocity response measured near the point of impact. The four locations included the center, one corner, and midlength on each side. The test allowed for identification of the actual resonance frequencies associated with the modeshapes in Fig. 2, except for $\mathbf{R}_1$, which either could not be excited adequately or was at a frequency above 200 Hz. Figure 3 shows the velocity spectra measured at each location, from which spectra the resonance frequencies could be determined.

4. COMPARISON OF EXPERIMENTAL AND FEM DATA

Resonance Frequencies. The measured and calculated resonance frequencies are summarized in Table 1. Several observations may be made:

- There is close agreement between the calculated and measured frequencies for modes $\mathbf{B}_1$, $\mathbf{B}_2$ and $\mathbf{B}_3$.
- The measured frequencies for modes T_1, T_2 and T_3 are 20 to 30 percent higher than those calculated using the FEM.
- The ratios between measured frequencies of modes $\mathbf{B}_1$, $\mathbf{B}_2$ and $\mathbf{B}_3$ are consistent with the corresponding published ratios for uniform free-free plates; the ratios between measured frequencies for modes T_1, T_2 and T_3 are approximately integers, more consistent with torsional vibration of a prismatic bar than with what would be expected with two-dimensional plate bending.

Predicting Slab Performance. It was desired to examine the feasibility of using finite element modeling to predict motions of the isolated slab on the basis of motions measured below the airsprings. Figure 4 compares the calculated and measured "transfer functions." A transfer function is defined as a spectrum of the ratio of the *displacement* at the top of the slab to the *displacement* at the base of the airsprings. A study indicated that realistic phase differences between the forcing loads at the base of the airsprings had relatively little effect on the calculated motions of the slab.

Corresponding transfer functions were obtained relating measured velocity of the slab surface to velocity of the bottom of the pit. The measured transfer function of Fig. 4 relates vertical motion at the center of the slab to vertical ground motion below the slab. The "FEM Vertical Only" curve represents the same quantity obtained using the model. There is fair correspondence between the curves at frequencies below about 70 Hz, but not at higher frequencies. The "FEM Geometric Mean" curve is the result of taking the geometric mean of the vertical response at the center and the corner of the slab to loading in the vertical and two horizontal directions, and then taking the geometric mean of those two curves.

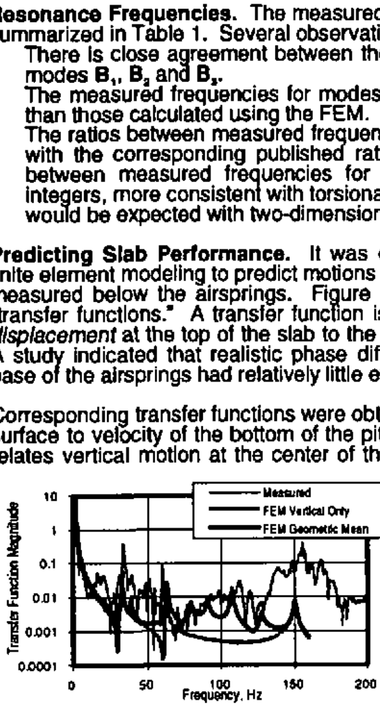

Figure 4. Measured and Calculated Transfer Functions

There is a better agreement with the measured data at frequencies below about 120 Hz, but the model does not predict the increased response above 120 Hz. (The behavior above 120 Hz is most likely due at least in part to deviation of the airsprings' behavior from that of an ideal linear massless spring or from disturbances that reach the slab through paths that do not involve the airsprings.) It appears that the motion of the system is subject to variables which cannot be adequately defined so that accurate finite element modeling of slab response to a realistic ground-motion input cannot be accomplished.

5. MEASURED SLAB PERFORMANCE

Ambient Vibrations. The root-sum-square (SRSS) velocity amplitude—summing the three velocity components at one point—was used to simplify the presentation of measured data in Fig. 5, which shows the SRSS velocity amplitude measured at the bottom of the pit (below the airsprings) and at two locations on the slab surface. The peaks at 1.4 Hz and 3 Hz are the result of resonance amplification associated with the mass on the airsprings, as expected.

As has been mentioned, the goal of the isolation system was to achieve a velocity of at most 0.75 μm/s at frequencies above 8 Hz. The measured SRSS velocity obtained at frequencies above 5 Hz is about 0.2 μm/s, well below the goal. The performance in this frequency range is limited by the amplitudes in the 31.5 Hz and 50 Hz one-third octave bands. If these were reduced by about three-quarters in future designs, the achieved velocity would be on the order of 0.08 μm/s, almost an order of magnitude below the original goal.

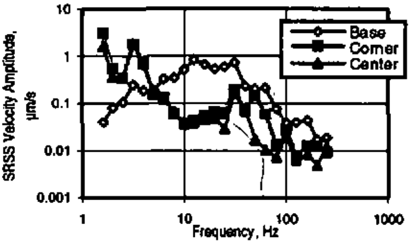

Figure 5. Measured Vibrations

Isolation System Performance. The peaks in the 31.5, 50 and 100 Hz bands are due to resonances of the slab. Figure 6 shows one measure of isolation system performance—the ratio between SRSS slab motion and SRSS base motion at the two measurement locations. It is evident that some degradation of isolation performance results from resonance amplification within the slab. The three peaks for which specific modes can be identified are marked. The reduced isolation at frequencies above 120 Hz is probably due to a combination of higher-order slab resonances and airspring nonlinearities.

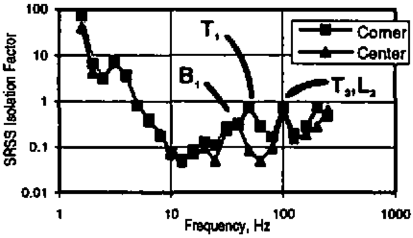

Figure 6. SRSS Vibration Isolation

6. CONCLUSIONS

This study documented the dynamic characteristics and vibration isolation performance of one of the largest isolation masses ever built for use in a laboratory environment. It also identified the extent to which finite element modeling could be used to predict behavior or a pneumatically supported system. The primary findings are summarized below.

- Finite element analysis (FEA) of the type used here can predict natural frequencies and mode shapes fairly well, but it does not predict bending and twisting modes with equal accuracy. Some improvement might be possible with a finer element mesh.
- FEA is inadequate for the prediction of response of an isolated slab to ground vibrations.
- Mass-airspring resonances can cause an order of magnitude or more amplification at the airspring resonance frequencies.
- Deviation of airspring behavior from that of an ideal massless spring may cause a significant degradation in isolation performance at frequencies above 100 Hz, perhaps by as much as two orders of magnitude.
- Slab resonances degrade isolation performance, perhaps by as much as an order of magnitude. These must be considered during design, and perhaps mitigated either by sizing the slab to achieve resonances above the frequency range of interest or by designing increased damping into the slab structure.